ALKU Journal of Science 2022, Sayı 4(2): 97-109
e-ISSN: 2667-7814

Original Article

Mixed Convection from Inclined Square Cylinder in a Square Cavity

Nazım Kurtulmuş*
Adana Alparslan Türkeş Bilim ve Teknoloji Üniversitesi, Mühendislik Fakültesi, Makine Mühendisliği Bölümü, Adana, Türkiye.
**nkurtulmus@atu.edu.tr*

Abstract

In this work, mixed convection from an inclined square cylinder in a cavity is numerically investigated. A commercial CFD solver Ansys Fluent is used to solve the problem. First, the inclined square cylinder is located at the center of the cavity, then the location of the cylinder is changed along the x-axis. The cavity walls are assumed to be adiabatic and the cylinder walls are assumed to be isothermal boundary condition. The Reynolds number, *Re* varies from 100 to 300 and the Grashof numbers, *Gr* range from 10^3 to 10^5 throughout the work. The working fluid is chosen as air at Prandtl number, Pr = 0.7. The Nusselt number, *Nu* variations, the distributions of velocity and isotherms are presented in Tables and Figures. The maximum Nusselt number, *Nu* is obtained as 11.47 at Re=300 and Gr = 10^3, 10^4 when the cylinder location is at the right place of the cavity.

Keywords: cavity, flow structure, heat transfer, mixed convection.

Kaviteye Yerleştirilen Açılı Kare Silindirden Doğal ve Zorlanmış Taşınım

Özet

Bu çalışmada, kavite içerisine yerleştirilmiş bir açı verilmiş kare silindirde meydana gelen doğal ve zorlanmış taşınım araştırılmıştır. Çözüm için ticari bir yazılım olan Ansys Fluent program kullanılmıştır. Silindir ilk etapta kavite merkezine yerleştirilmiş, daha sonra ise kavite içerisinde x ekseni boyunca farklı konumlarda bulundurulmuştur. Kavite duvarları yalıtılmış, silindir duvarları ise belli bir sıcaklıkta tutulduğu kabul edilmiştir. Reynolds sayısı 100'den 300' e, Grashof sayısı ise 10^3' den 10^5' e kadar değişmektedir. Çalışma akışkanı olarak 0,7 Prandtl sayısındaki özelliklere sahip hava tercih edilmiştir. Nusselt sayısındaki değişim, hız ve sıcaklık izotermlerindeki dağılımlar şekiller ve tablolar vasıtasıyla sunulmuştur. Maximum Nusselt sayısı Re sayınının 300 ve Gr sayısının 10^3, 10^4 değerlerinde, silindir konumunun kavitenin sağ kısmında bulunduğu durumda 11,47 olarak elde edilmiştir.

Anahtar kelimeler: akış yapısı, doğal ve zorlanmış taşınım, ısı transferi, kavite.

Geliş/Received: 23 Ağu 2022/23 Aug 2022
Kabul Ediliş/Accepted: 29 Ağu 2022/29 Aug 2022

1. INTRODUCTION

The mixed convection from a square cylinder is mostly encountered in engineering applications such as cooling electronic equipment, solar collectors, etc. In this context, the topic of mixed convection from a hot cylinder placed in the square cavity attracts the attention of researchers. Chamkha et al. [1] conducted a numerical study to investigate the heat transfer and flow characteristics of a square cylinder placed in a square cavity. They implied different inlet/ outlet configurations to figure out the thermal characteristics. The Richardson number, *Ri* and Reynolds numbers, *Re* varies from 0 to 10 and 50 to 200, respectively. The results showed that the average Nusselt number, *Nu* of square cylinder upgrades as the Richardson and the Reynolds numbers rise. Mamun et al. [2] numerically investigated mixed convection in a square cavity in the presence of a hollow heated cylinder. The cavity was ventilated, while the walls of the cavity were adiabatic. Also, the cylinder diameter varied. They concluded that the maximum Nusselt number was obtained when the diameter of the cylinders was largest. Laidoudi [3] studied the heat transfer characteristics of two heated circular cylinders placed in a square enclosure. They claimed that the average Nusselt number, *Nu* increases with increasing Ri and Re numbers in the range of the study. Ali and Jalal [4] investigated natural convection from two heated circular cylinders placed in a square enclosure with different inlet and outlet ports. Both the locations of the cylinders and the inlet/outlet ports varied throughout the study, and it was seen that both of them were significant parameters that effect on the heat transfer rates. Mehrizi et al. [5] investigated mixed convection from an obstacle in a cavity in the case of the usage of nanofluid as a working fluid. The effect of the location of the inlet /outlet ports of the cavity was also examined. The Ri number varied from 0.1 to 10 and Grashof number, *Gr* was taken as 10^4. Generally, using nanofluid as a working fluid increases the heat transfer rates; moreover, increasing the volume fraction of nanoparticles contributes to heat transfer. There are more works on hot bodies placed in a cavity [6-12].

Furthermore, researchers implied active and passive heat transfer enhancement techniques to upgrade convection in a vented cavity. Jasim et al. [13] conducted a numerical study by implying rotation to the cylinder placed in a vented cavity using a hybrid nanofluid as a working fluid. The diameter and location of the cylinder also were varied. Gr numbers range from 10^3 to 10^5 and Reynolds range from 50 to 500. Their results showed that 21% heat transfer enhancement could be reached. Hamzah et al. [14] researched the mixed convection from a heated cylinder located near the two counter-rotating cylinders in a cavity. They calculated a maximum heat transfer enhancement of 20.9%. Moayedi [15] investigated heat transfer from double-rotating cylinders in a cavity with different locations. Also, the variations of inlet and outlet ports were examined. The results showed that if the rotation direction is counterclockwise, a higher heat transfer rate was obtained than clockwise rotation. The average Nusselt number was enhanced as 56.03% with an optimum configuration. Additionally, magnetic field were also implied to improve heat transfer in cavities [16, 21]. Time-varied flow at the inlet of the cavity was applied to enhance the heat transfer rates in the literature [22,23].

This study investigates mixed convection from an inclined square cylinder in a square cavity. The location of the inclined square cylinder varies along the x-axis. The effect of Grashof number, *Gr* and Reynolds numbers, *Re* variations on the heat transfer and flow pattern is examined.

2. SYSTEM DESCRIPTIONS

2.2 Model Geometry

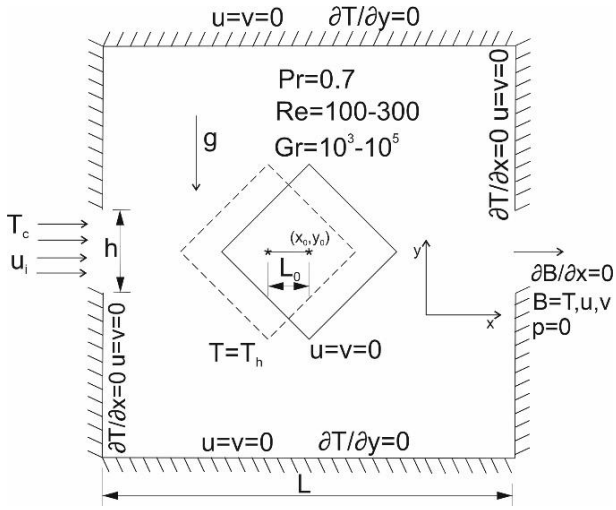

Figure 1. The schematic representations of the model

Figure 1 shows the schematic representations of the model geometry investigated. The center of the inclined square cylinder is located at the origin (x_0, y_0) of the Cartesian coordinate system in the case of L_0=0. Two other cases were examined, such as L_0=L/10 and L_0=-L/10. L represents the one-side length of the square cavity. The central axis of the inlet and outlet ports are symmetrical considering the center of the Cartesian coordinate system and their length, *h* is taken as L/5. The walls of the cavity are assumed as adiabatic. The air as a working fluid enters the cavity from the inlet section uniformly at cold temperature, T_c. The inclined square cylinders are heated and their walls are kept at a hot temperature, T_h. The length of one side of the inclined square cylinder is taken as L/2.5. No-slip has implied all the walls of the cavity and inclined square cylinder.

2.2 Governing equations and solution procedure

In this work, the flow is assumed as laminar, two-dimensional, incompressible and at a steady state. Pr number is taken as 0.7. The thermophysical properties of the working fluid are constant, except the density. Boussinesq approximation was applied to the density of the working fluid. In addition, radiation and viscous dissipation are insignificant. The governing equations are as follows,

Continuity equation,

$$\frac{\partial u}{\partial x}+\frac{\partial v}{\partial x}=0 \tag{1}$$

Momentum equations,

$$u\frac{\partial u}{\partial x}+v\frac{\partial u}{\partial y}=-\frac{1}{\rho}\frac{\partial p}{\partial x}+\frac{\mu}{\rho}\left(\frac{\partial^2 u}{\partial x^2}+\frac{\partial^2 u}{\partial y^2}\right) \tag{2}$$

$$u\frac{\partial v}{\partial x}+v\frac{\partial v}{\partial y}=-\frac{1}{\rho}\frac{\partial p}{\partial x}+\frac{\mu}{\rho}\left(\frac{\partial^2 v}{\partial x^2}+\frac{\partial^2 v}{\partial y^2}\right)+\beta g(T-T_c) \tag{3}$$

Energy equation,

$$\left(u\frac{\partial T}{\partial x}+v\frac{\partial T}{\partial y}\right)=a\left(\frac{\partial^2 T}{\partial x^2}+\frac{\partial^2 T}{\partial y^2}\right) \tag{4}$$

where $a = k/\rho c_p$' dir.

The dimensionless parameters are as follows,

X=x/L, Y=y/L, $\theta = \frac{T-T_c}{T_h-T_c}$, $Re = \frac{u_i L}{\vartheta}$, $Gr = \frac{g\beta(T_h-T_c)L^3}{\vartheta^2}$, Pr = ϑ / a

The local Nusselt number, Nu_y can be calculated as follows,

$$Nu_y = -\left(\frac{\partial\theta}{\partial Y}\right)_{Y=0} \quad (5)$$

The average Nusselt number, Nu_{avg} can be calculated as follows,

$$Nu_{avg} = \frac{1}{L}\int_{X=0}^{X=L} Nu_y dX \quad (6)$$

The boundary conditions at the inlet are U=1, V=0 and $\theta = 0$

The boundary conditions at the outlet are $\frac{\partial U}{\partial X} = 0$, $\frac{\partial V}{\partial X} = 0$ and $\frac{\partial \theta}{\partial X} = 0$ and P=0

The boundary conditions at the cavity wall are U=0, V=0 and $\frac{\partial \theta}{\partial X} = 0$

The boundary conditions for an inclined square cylinder are U=0, V=0 and $\theta = 1$

A commercial CFD solver Ansys Fluent [24] is used to solve the problem. The finite volume technique was applied. A simple algorithm was selected. Second order upwind technique was used to discretized equations 1-4. Consequently, iterations were carried on until convergence criteria 1 x10 $^{-8}$ were reached.

The mesh used in the study and the element type is illustrated in Fig. 2. In this figure, 20372 triangular elements with 11506 nodes are used. The mesh type and nodes are acceptable and verify the accuracy. Furthermore, a validation study was conducted. It was noted that the current study results agreed with the results by Lee et al. [25], who performed an analysis to investigate the convection from a heated circular cylinder in a cavity. The hot cylinder was located in a square enclosure in their study. The walls were in isothermal conditions. In the validation case, Rayleigh's number was taken as 10^5. They found the mean Nusselt number as 7.76. When the same boundary conditions were applied in the current study, the mean Nusselt number was obtained as 7.86 with a 1% difference.

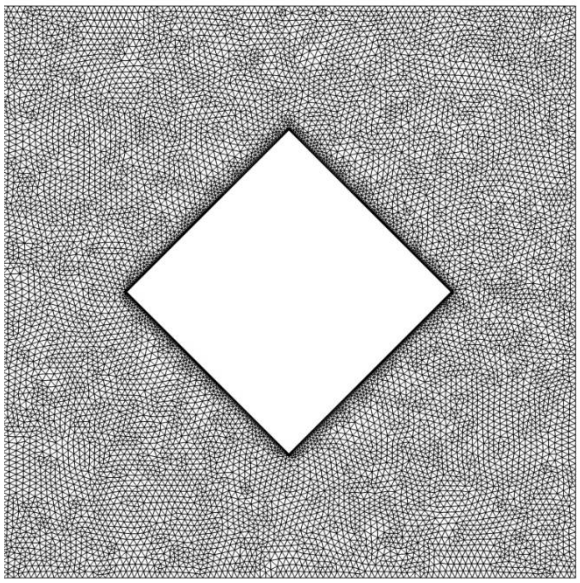

Figure 2. The triangular mesh distribution

3. RESULTS AND DISCUSSION

Table 1 indicates the Nusselt number, Nu variation with increasing Reynolds number, Re at Gr = 10^3. As seen, the Nusselt number is sensitive to the displacement of the inclined square cylinder in the cavity. The Nusselt number first decreases then increase as the body moves from left to right for all Reynolds numbers, *Re*. L_0 = L/10 and L_0= - L/10 represent the right and left positions of the cylinders in the cavity, respectively. It is noted that the Nu number is higher in the case of L_0=L/10 than in the case of L_0= - L/10. The highest heat transfer rate is taken place in the case of L_0= - L/10 at the Reynolds number of 300. As can be seen, the heat transfer upgrades with increasing Reynolds numbers. The effect of the increment Grashof number, *Gr* is evaluated in Tables 2 and 3. While any significant changes are taken place in the case of Gr =10^4, the deterioration of heat transfer rates from the cylinders in the cavity stands out in the case of Gr =10^5. At the Reynolds number of 100 and the location of L_0=0, the deterioration reaches 28% in the case of Gr =10^5 compared to the case of Gr= 10^4. The lowest Nusselt number, *Nu* is obtained as 4.66 for Re =100 at the cylinder's position of L_0=0. When the Reynolds number increases, the forced flow dominates flow structures in the cavity and consequently, the heat transfer rates upgrades. With this context, the increase rate attains 129% from 80% in the case of L_0=L/10 when the Grashof number increases from Gr = 10^3 to Gr = 10^5.

Table 1. Nu number, *Nu* variation with increasing Re number (Gr = 10^3)

Re	Nu (L_0= - L/10)	Nu (L_0=0)	Nu (L_0=L/10)
100	6.32	6.16	6.37
200	9.16	8.97	9.43
300	11.06	10.79	11.47

Table 2. Nu number, *Nu* variation with increasing Re number (Gr = 10^4)

Re	Nu (L_0= - L/10)	Nu (L_0=0)	Nu (L_0= L/10)
100	6.32	6.09	6.29
200	9.17	8.96	9.42
300	11.06	10.79	11.47

Table 3. Nu number, *Nu* variation with increasing Re number (Gr = 10^5)

Re	Nu (L_0= - L/10)	Nu (L_0=0)	Nu (L_0= L/10)
100	5.72	4.66	4.79
200	9.19	8.11	8.63
300	11.14	10.68	11.34

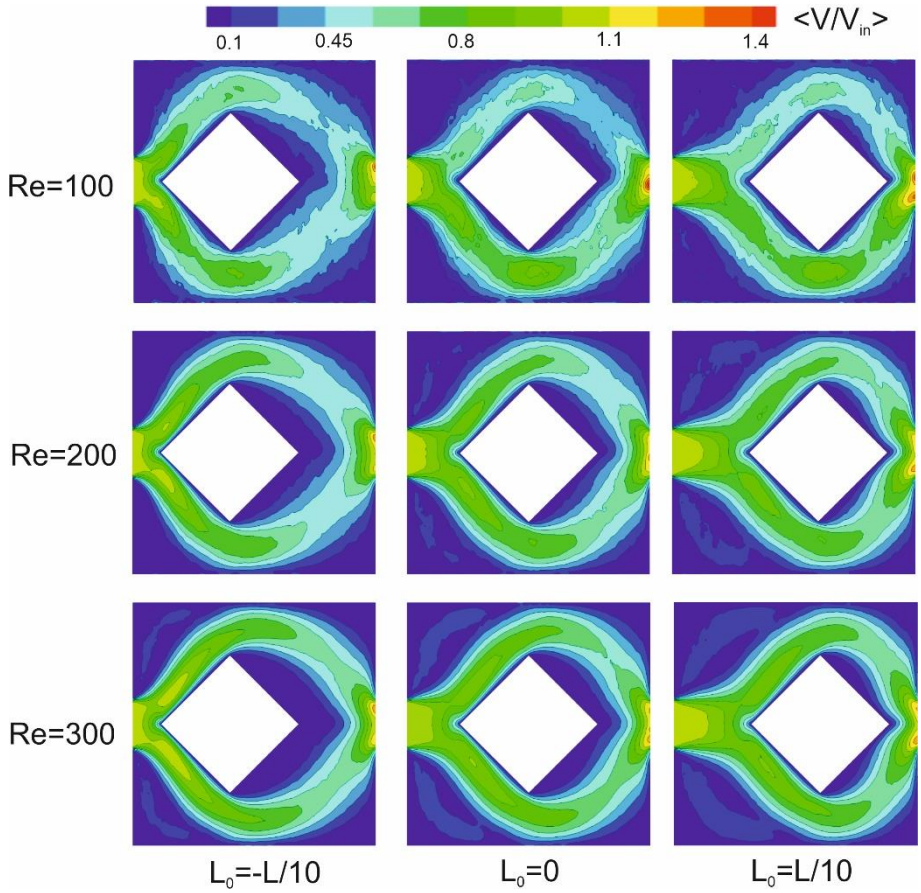

Figure 3. Velocity distributions for different configurations at Gr =10^3

The distribution of velocity in the cavity with the presence of the inclined square cylinder is seen in Figure 3 for different locations of the body at Gr = 10^3. The magnitudes of the $<V/V_{in}>$ can be followed by the legend at the top. When the dark blue contours represent the minimum values, the dark red represents the maximum values. The symmetry concerning the center of the cylinder in the flow pattern is seen. The flow splits when it enters the cavity from the inlet port. The bifurcated fluid follows almost the same trajectory at both sides of the inclined square cylinder and exits from the outlet port of the cavity. Besides, recirculation regions near the upper and lower corners of the cavity are formed when the fluid enters the cavity. The recirculation regions enlarge in size and the severity increases when the Reynolds numbers rise in all cases. Moreover, additional recirculating regions are taken place on the right sides of the cylinder in the cavity when the Reynolds number reaches the value of 300. The aforementioned regions occupy more area when the inclined square cylinders move from left to right.

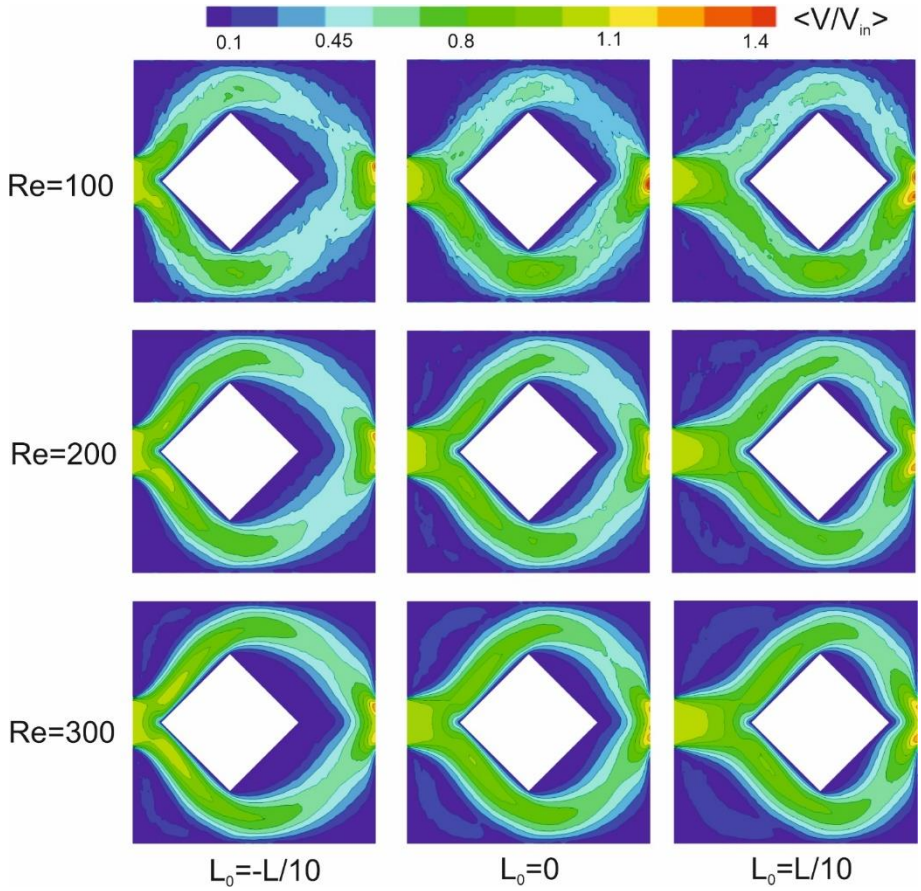

Figure 4. Velocity distributions for different configurations at Gr =10^4

The effect of the increase in the number of Grashof numbers, *Gr* has begun to be seen in Figure 4, especially for low Reynolds numbers. Some incoming flow is forced to the bottom side of the inclined square cylinders compared to the upper sides of the cavity at the Reynolds number of 100. However, the forced convection becomes dominant as Reynolds number increases. Namely, the symmetrical velocity distribution is taken place. The recirculating regions still exist in vicinity of the right sides of the cylinder in the cavity when the Reynolds number reaches the value of 300. It is notes they are the symmetrical concerning the center of the square cavity. These recirculating regions shrink in size when the inclined square cylinders move from left to right location of the cavity.

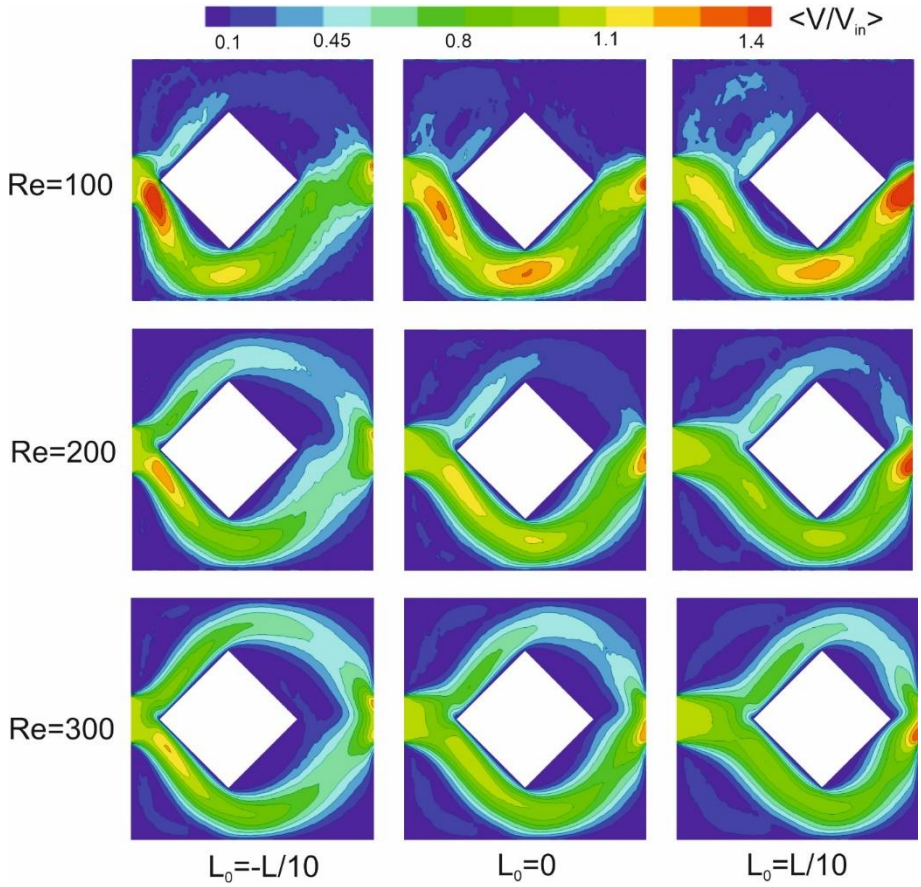

Figure 5. Velocity distributions for different configurations at Gr =10^5

The bouncy force becomes dominant at a lower Reynolds number, as seen in Figure 5. The recirculation region near the upper sides of the cavity forces the fluid to flow to the bottom side of the cavity. Almost all the fluid flows throughout the bottom side since the fluid is trapped at the upper region resulting higher pressure. Hence, the heat transfer from the top side of the inclined square cylinder decreases. It is noted there is another recirculating region near the outlet port at the upper side of the cavity. Due to the bouncy forces, a small recirculation is situated in the vicinity of the bottom side of the cylinder. On the other hand, the symmetry that was present in previous Gr numbers at Reynolds number of 300 is disappear in this case. The recirculating region near the entrance at the upper side of the cavity enlarges when the body moves from left to right. However, as the momentum of the fluid increases, fluid flows in the vicinity of the upper side of the cylinder, especially at the Reynolds number of 300. The recirculating regions taken place in the cavity are forced to shrink in size by the main flow region.

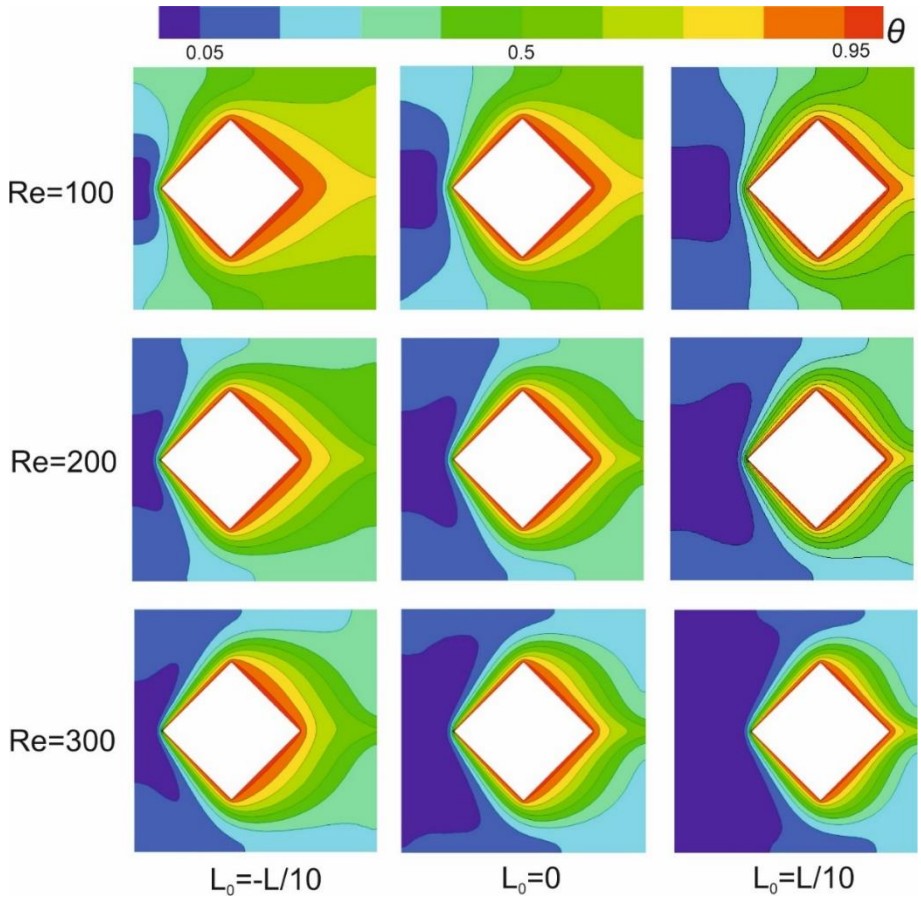

Figure 6. The distribution of isotherms for different configurations at Gr =10^3

Figure 6 depicts the distribution of isotherms for the inclined square cylinder in the cavity at Gr =10^3. The distribution of the isotherms is symmetrical concerning the center of the cylinder in all cases. The thermal boundary layer is thinner on the left side than on the right side due to the fluid with high momentum at the front side of the cylinder. Additionally, the thermal boundary layer becomes thinner as the Reynolds number increases. The cylinder locations are essential in terms of the temperature distribution of the cavity. This occasion is also valid for the Reynolds number increments. When the Reynolds number increases, the isotherms with high values occupies lower region comparatively in the cavity.

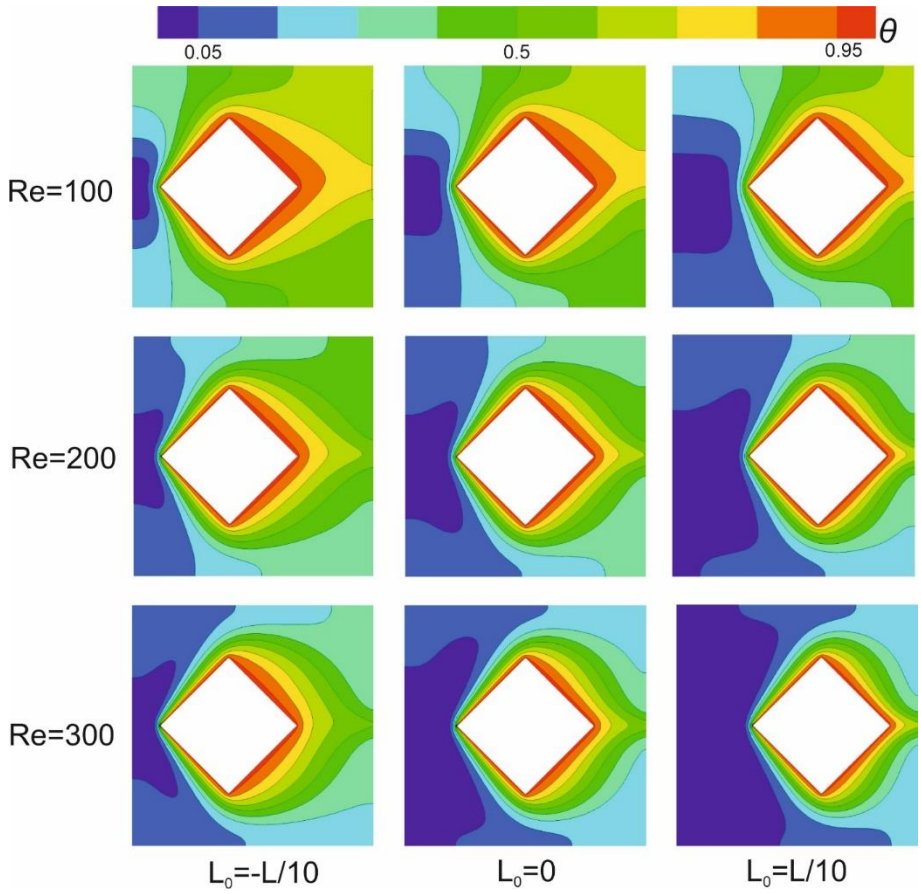

Figure 7. the distribution of isotherms for different configurations at Gr =10^4

Figure 7 reveals the contour of the isotherms in the cavity at Gr =10^4. The effect of the Grashof number, *Gr* emanates especially for low Reynolds numbers. The symmetrical distribution of isotherms is dissipated in the cavity. With an increase in the Reynolds number, the symmetrical distribution is restored. Figure 8 depicts the patterns of the isotherms in the cavity at Gr =10^5. The asymmetry is clearly seen from the contours of the temperature in the cavity at the Reynolds number of 100. Since the fluid is trapped at the upper sides of the cavity, the heat transfer rates deteriorate in this case. However, the heat transfer rates increase as the flow momentum increases with a higher Reynolds number, *Re*. The thermal boundary layer gets thinner as flow momentum rises.

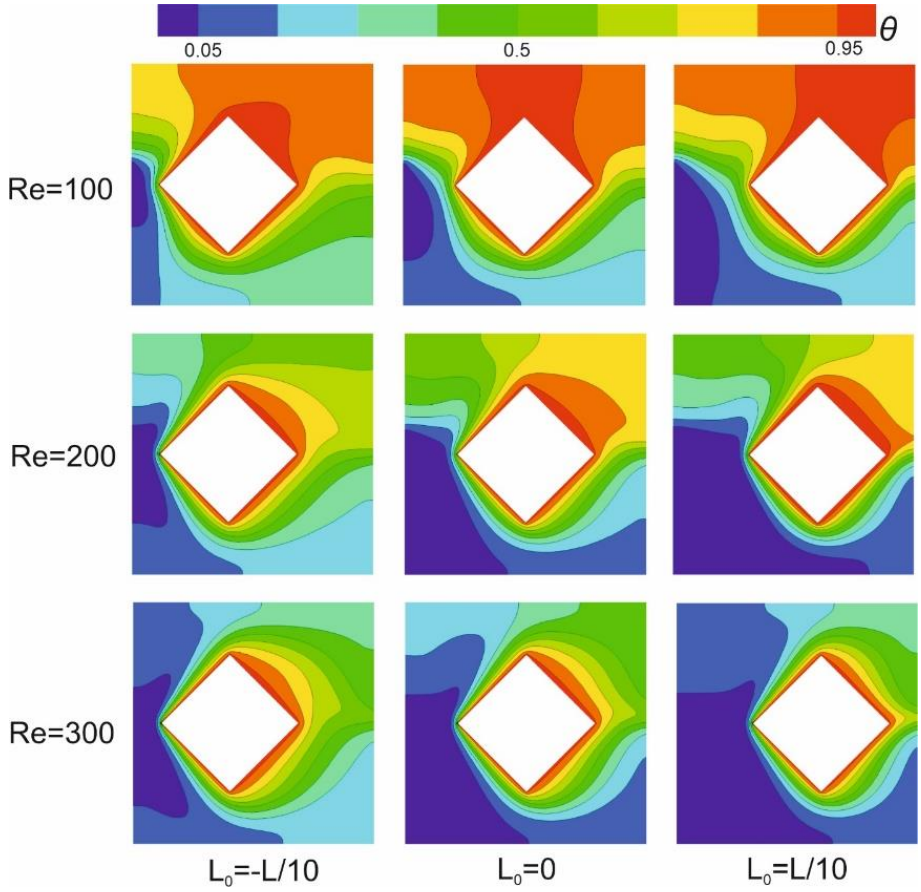

Figure 8. The distribution of isotherms for different configurations at Gr =10^5

4. CONCLUSION

The heat transfer characteristics and flow structures are evaluated to investigate the mixed convection from an inclined square cylinder in a cavity. A commercial CFD solver Ansys Fluent is utilized to perform the analysis. The results showed that while the bouncy forces considerably affect the flow structures at low Reynolds numbers, forced convection becomes dominant when the Reynolds number increases. Reynolds number is an important parameter that affects the heat transfer rates remarkably. For example, when the Reynolds number increases from 100 to 300, the heat transfer rate attains 129% in the case of Gr=10^5. While the maximum average Nusselt number, *Nu* is obtained as 11.47 for the case of L_0= L/10, the minimum average Nusselt number is obtained as 4.66 for the case of L_0=0. In addition, the inclined square cylinder's location in a cavity considerably affects the flow patterns. For instance, the Nusselt number is 5.72 in the case of L_0= - L/10. However, it declines about 18% and becomes 4.66 in the case of L_0= 0 at Re=100 and Gr = 10^5.

REFERENCES

[1] Ali J. Chamkha, Salam Hadi Hussain & Qusay Rashid Abd-Amer (2011). "Mixed Convection Heat Transfer of Air inside a Square Vented Cavity with a Heated Horizontal Square Cylinder." Numerical Heat Transfer, Part A: Applications 59 (1), 58-79. DOI: 10.1080/10407782.2011.541216

[2] M.A.H. Mamun, M.M. Rahman, M.M. Billah, R. Saidur (2010). "A numerical study on the effect of a heated hollow cylinder on mixed convection in a ventilated cavity." International Communications in Heat and Mass Transfer 37 (9), 1326-1334. https://doi.org/10.1016/j.icheatmasstransfer.2010.07.019.

[3] H. Laidoudi (2020). "Upward flow and heat transfer around two heated circular cylinders in square duct under aiding thermal buoyancy." Journal of the Serbian Society for Computational Mechanics 14(1), 113-123. DOI: 10.24874/jsscm.2020.14.01.10.

[4] Mahmud H. Ali, Rawand E. Jalal (2020). "Natural convection in a square enclosure with different openings and involves two cylinders: A numerical approach." Frontiers in Heat and Mass Transfer 15(1), 27. DOI: 10.5098/hmt.15.27.

[5] A. Abouei Mehrizi, M. Farhadi, H. Hassanzade Afroozi, K. Sedighi, A.A. Rabienataj Darz (2012). "Mixed convection heat transfer in a ventilated cavity with hot obstacle: Effect of nanofluid and outlet port location." International Communications in Heat and Mass Transfer 39 (7), 1000-1008. https://doi.org/10.1016/j.icheatmasstransfer.2012.04.002.

[6] Md. Mustafizur Rahman, Salma Parvin, Md. Hasanuzzaman, Rahman Saidur & Nasrudin A. Rahim (2013). "Effect of Heat-Generating Solid Body on Mixed Convection Flow in a Ventilated Cavity." Heat Transfer Engineering 34 (15), 1249-1261. https://doi.org/10.1080/01457632.2013.730919.

[7] Fariborz Karimi, Hongtao Xu, Zhiyun Wang, Mo Yang & Yuwen Zhang (2016). "Numerical Simulation of Steady Mixed Convection Around Two Heated Circular Cylinders in a Square Enclosure." Heat Transfer Engineering 37, 64-75. DOI: 10.1080/01457632.2015.1042343.

[8] M.M. Rahman, S. Parvin, N.A. Rahim, M. Hasanuzzaman, R. Saidur (2012). "Simulation of mixed convection heat transfer in a horizontal channel with an open cavity containing a heated hollow cylinder." Heat Transfer—Asian Research 41, 339-353. https://doi.org/10.1002/htj.21002.

[9] O.M. Ali (2022). "Effect of Horizontal Spacing on Natural Convection Heat Transfer from Two Aligned Horizontal Cylinders in a Vented Enclosure." Arabian Journal for Science and Engineering 47, 8257–8272. https://doi.org/10.1007/s13369-021-06259-2.

[10] Omar Mohammed Ali, Omar Rafae Alomar (2021). "Mixed convection heat transfer from two aligned horizontal heated cylinders in a vented square enclosure." Thermal Science and Engineering Progress 25, 101041. https://doi.org/10.1016/j.tsep.2021.101041.

[11] Ali Omar M., Mahmood Raid A., Al-Brifkani Mohammed W (2022). "Augmentation of convection heat transfer from a horizontal cylinder in a vented square enclosure with variation of lower opening size." Thermal Science 26 (3), 2027-2041. https://doi.org/10.2298/TSCI201119176A.

[12] T.V. Radhakrishnan, A.K. Verma, C. Balaji, S.P. Venkateshan (2007). "An experimental and numerical investigation of mixed convection from a heat generating element in a ventilated cavity." Experimental Thermal and Fluid Science 32 (2), 502-520. https://doi.org/10.1016/j.expthermflusci.2007.06.001.

[13] Laith M. Jasim, Hudhaifa Hamzah, Cetin Canpolat, Besir Sahin (2021). "Mixed convection flow of hybrid nanofluid through a vented enclosure with an inner rotating cylinder." International Communications in Heat and Mass Transfer 121, 105086. https://doi.org/10.1016/j.icheatmasstransfer.2020.105086.

[14] Hudhaifa Hamzah, Cetin Canpolat, Laith M. Jasim, Besir Sahin (2021). "Hydrothermal index and entropy generation of a heated cylinder placed between two oppositely rotating cylinders in

a vented cavity." International Journal of Mechanical Sciences 201, 106465. https://doi.org/10.1016/j.ijmecsci.2021.106465.

[15] Hesam Moayedi (2021). "Investigation of heat transfer enhancement of Cu-water nanofluid by different configurations of double rotating cylinders in a vented cavity with different inlet and outlet ports." International Communications in Heat and Mass Transfer 126, 105432. https://doi.org/10.1016/j.icheatmasstransfer.2021.105432.

[16] Harun Zontul, Hudhaifa Hamzah, Besir Sahin (2021). "Impact of periodic magnetic source on natural convection and entropy generation of ferrofluids in a baffled cavity." International Journal of Numerical Methods for Heat & Fluid Flow 31 (12), 3547-3575. https://doi.org/10.1108/HFF-10-2020-0671.

[17] Fatih Selimefendigil, Hakan F. Öztop (2022). "Thermal management and performance improvement by using coupled effects of magnetic field and phase change material for hybrid nanoliquid convection through a 3D vented cylindrical cavity." International Journal of Heat and Mass Transfer 183, 122233. https://doi.org/10.1016/j.ijheatmasstransfer.2021.122233.

[18] B. Pekmen Geridönmez, H.F. Öztop (2021). "Effects of partial magnetic field in a vented square cavity with aiding and opposing of MWCNT–water nanofluid flows." Engineering Analysis with Boundary Elements 133, 84-94. https://doi.org/10.1016/j.enganabound.2021.08.024.

[19] Fatih Selimefendigil, Hakan F. Öztop (2019). "Fluid-solid interaction of elastic-step type corrugation effects on the mixed convection of nanofluid in a vented cavity with magnetic field." International Journal of Mechanical Sciences 152, 185-197. https://doi.org/10.1016/j.ijmecsci.2018.12.044.

[20] A. Purusothaman, H.F. Oztop, N. Nithyadevi, Nidal H. Abu-Hamdeh (2016). "3D natural convection in a cubical cavity with a thermally active heater under the presence of an external magnetic field." Computers & Fluids 128, 30-40. https://doi.org/10.1016/j.compfluid.2016.01.011.

[21] Aissa Abderrahmane, Umar F. Alqsair, Kamel Guedri, Wasim Jamshed, Nor Ain AzeanyMohd Nasir, Hasan Sh. Majdi, Shaghayegh Baghaei, Abed Mourad, Riadh Marzouki, (2022). "Analysis of mixed convection of a power-law non-Newtonian nanofluid through a vented enclosure with rotating cylinder under magnetic field." Annals of Nuclear Energy 178,109339. https://doi.org/10.1016/j.anucene.2022.109339.

[22] Fatih Selimefendigil, Hakan F. Öztop (2014). "Numerical investigation and dynamical analysis of mixed convection in a vented cavity with pulsating flow." Computers & Fluids 91, 57-67. https://doi.org/10.1016/j.compfluid.2013.11.033.

[23] Fatih Selimefendigil, Hakan F. Öztop (2015). "Effects of phase shift on the heat transfer characteristics in pulsating mixed convection flow in a multiple vented cavity." Applied Mathematical Modelling 39 (13), 3666-3677. https://doi.org/10.1016/j.apm.2014.11.065.

[24] Fluent A.N.S.Y.S (2018), "ANSYS fluent manual.

[25] J.M. Lee, M.Y. Ha, H.S. Yoon (2010). "Natural convection in a square enclosure with a circular cylinder at different horizontal and diagonal locations." International Journal of Heat and Mass Transfer 53, 5905-5919. https://doi.org/10.1016/j.ijheatmasstransfer.2010.07.043.